Electronic Supplementary Material (ESI) for Materials Advances.

Simulating excited states in metal organic frameworks: From light-absorption to photochemical CO_2 reduction: Supplementary Information

Michael Ingham, Alex Aziz, Devis Di Tommaso, and Rachel Crespo-Otero

Contents

S1 Computational details

The relaxed (KS-DFT/PBE-D3BJ) unit cell of QMOF-d29cec2 was obtained from the QMOF database. We performed single-point periodic DFT calculations using the PBE, PBE0, B3LYP, and HSE06 functionals as implemented in VASP6.4.0, to determine the fundamental band gap, E_g.[1] The PBE projector augmented wave (PAW) potentials were used, with a plane-wave energy cut-off of 520 eV. The Brillouin zone was sampled using a $2 \times 2 \times 2$ Monkhorst-Pack k-point grid. Subsequently, the Sumo program[2] was used to generate a suitable k-point path ($\Gamma \rightarrow Z \rightarrow Y \rightarrow \Gamma \rightarrow X \rightarrow V \rightarrow R \rightarrow U$) for which an electronic band structure calculation was carried out with a cut-off of 520 eV at the HSE06-level.

From the relaxed unit cell, we constructed six cluster models of increasing size (Fig. S1). The smallest model (Model 1) consists of just of a Zn_4O node bonded to the terminal $-CO_2-$ groups of the organic linker, whereas the largest model (Model 6) includes the full coordination sphere. Models 2 to 4 contain two of each linker type, and Model 5 includes a one of each linker type. For each cluster model, we selected bond cuts at the C-C adjacent to the M-L boundary, instead of the Zn-O itself, to avoid cutting dative bonds. We terminated the dangling bonds with hydrogen link atoms along the vector of the bond cuts.[3] We then relaxed the link atoms (KS-DFT/PBE-D3BJ/TZVP) whilst keeping the positions of all other atoms in the cluster fixed. Additionally, for the ONIOM calculations, we constructed a large *real* region consisting of seven nodes and 40 linkers capped with hydrogen link atoms (Fig. S2). All geometries are visualised using Mercury.[4]

On each of these cluster models, the first five excited states of each model were calculated using the PBE, PBE0, B3LYP, HSE06, and ωB97X-D functionals: 1) TDDFT/TZVP calculations, with Gaussian16;[5] 2) ONIOM(TDDFT/TZVP:PM6)-EE, as implemented in Gaussian09;[6] 3) BSE/RI-evGW/DFT/def2-TZVP calculations, as implemented in Turbomole7.6.[7] We used Gaussian09 for the ONIOM calculations to allow electronic embedding at the QM/QM' level. We did not perform calculations for the HSE06 functional for the GW calculations. E_g and E_{opt} were determined from each. Finally, RI-evGW/DFT/def2-TZVP calculations were used to determine the quasiparticle gap for each DFT molecular orbital, as implemented in Turbomole7.6, followed by BSE/evGW/DFT to calculate the first five excited states. For the isolated TDDFT calculations, frontier orbital (HOMO and LUMO) were obtained using the `cubegen` program in Gaussian16, and were visualised using VMD.[8] Finally, we used the `cubman` program in Gaussian16 to generate density differences between the ground and first three excited states, visualised using VMD.

S2 Cluster models

These models were used for the isolated cluster calculations. For the ONIOM-EE calculations, the clusters (without link atoms) were used as the *model* region.

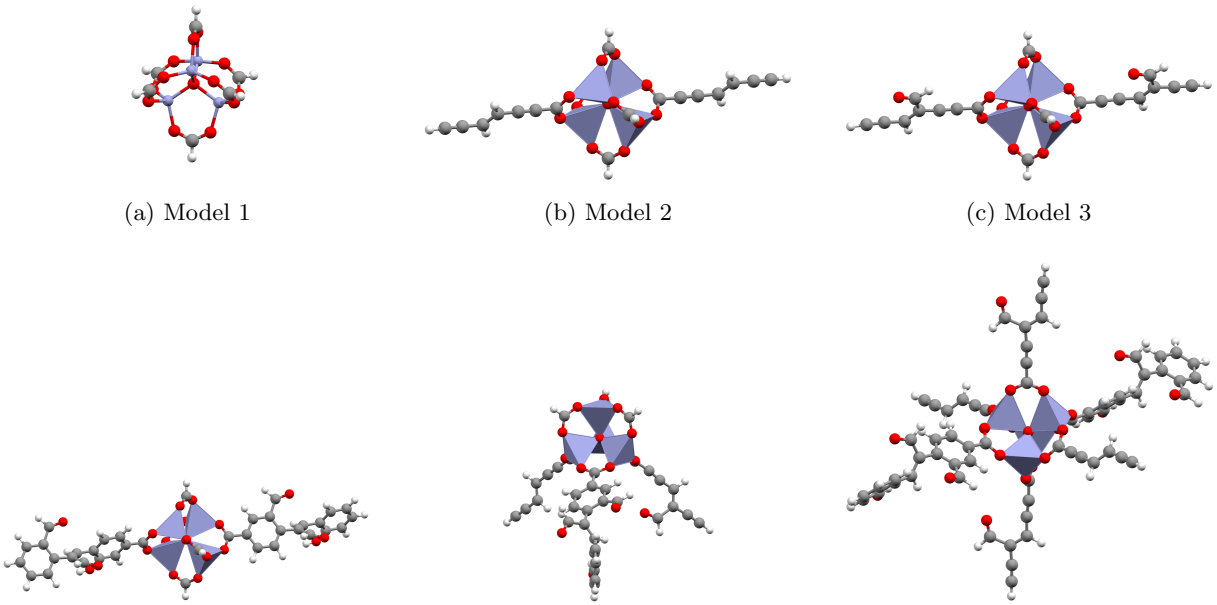

(a) Model 1 (b) Model 2 (c) Model 3

(d) Model 4 (e) Model 5 (f) Model 6

Figure S1: Cluster models

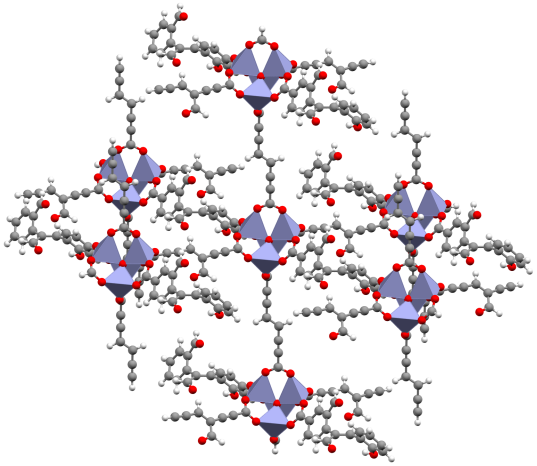

Figure S2: ONIOM-EE real region

S3 Excited-state energies and oscillator strengths

S3.1 Isolated cluster model calculations

Table S1: TDDFT/TZVP excitation energies and oscillator strengths for the first three excited-states, calculated using Gaussian16

Model	Functional	S1		S2		S3	
Model 1	PBE	5.10	f=0.0002	5.13	f=0.0003	5.18	f=0.0005
	PBE0	6.19	f=0.0000	6.25	f=0.0000	6.28	f=0.0000
	HSE06	6.18	f=0.0000	6.23	f=0.0001	6.27	f=0.0000
	B3LYP	6.08	f=0.0000	6.14	f=0.0001	6.17	f=0.0000
	ωB97x-D	6.27	f=0.0000	6.32	f=0.0000	6.36	f=0.0000
Model 2	PBE	2.61	f=0.0005	3.42	f=0.0003	3.44	f=0.0005
	PBE0	4.07	f=0.0058	4.08	f=0.0000	4.13	f=0.0027
	HSE06	3.65	f=0.0004	4.01	f=0.0000	4.04	f=0.0054
	B3LYP	3.81	f=0.0007	3.94	f=0.0000	3.97	f=0.0049
	ωB97x-D	4.31	f=0.0218	4.41	f=1.1085	4.42	f=0.0005
Model 3	PBE	2.27	f=0.0001	2.28	f=0.0000	2.32	f=0.0002
	PBE0	2.92	f=0.0002	3.13	f=0.0002	3.86	f=0.0826
	HSE06	2.90	f=0.0002	3.11	f=0.0002	3.35	f=0.0002
	B3LYP	2.86	f=0.0001	3.08	f=0.0002	3.54	f=0.0006
	ωB97x-D	3.17	f=0.0002	3.34	f=0.0002	4.07	f=1.1630
Model 4	PBE	1.89	f=0.0000	2.18	f=0.0000	2.22	f=0.0953
	PBE0	2.97	f=0.2352	3.04	f=0.1751	3.20	f=0.0054
	HSE06	2.89	f=0.2175	2.90	f=0.0023	3.00	f=0.1977
	B3LYP	2.85	f=0.2176	2.95	f=0.1998	3.08	f=0.0139
	ωB97x-D	3.29	f=0.1490	3.31	f=0.0794	3.67	f=0.1476
Model 5	PBE	1.65	f=0.0000	1.94	f=0.0000	2.18	f=0.0004
	PBE0	2.97	f=0.1899	3.09	f=0.0001	3.13	f=0.0002
	HSE06	2.62	f=0.0001	2.89	f=0.1820	3.05	f=0.0001
	B3LYP	2.79	f=0.0013	2.85	f=0.1770	3.08	f=0.0152
	ωB97x-D	3.29	f=0.1057	3.34	f=0.0003	3.67	f=0.0990
Model 6	PBE	1.54	f=0.0000	1.68	f=0.0001	1.82	f=0.0000
	PBE0	2.93	f=0.0002	2.98	f=0.2264	3.01	f=0.0046
	HSE06	2.50	f=0.0001	2.65	f=0.0001	2.82	f=0.0003
	B3LYP	2.71	f=0.0002	2.82	f=0.0027	2.86	f=0.2104
	ωB97x-D	3.18	f=0.0002	3.29	f=0.1474	3.30	f=0.0813

S3.2 ONIOM calculations

Table S2: ONIOM(TDDFT/TZVP:PM6) excitation energies and oscillator strengths for the first three excited states, calculating using Gaussian09.

Model	Functional	S1		S2		S3	
Model 1	PBE	5.09	f=0.0006	5.12	f=0.0008	5.16	f=0.0011
	PBE0	6.18	f=0.0000	6.24	f=0.0001	6.25	f=0.0000
	HSE06	6.16	f=0.0001	6.22	f=0.0001	6.24	f=0.0000
	B3LYP	6.06	f=0.0001	6.12	f=0.0002	6.14	f=0.0000
	ωB97x-D	6.26	f=0.0000	6.31	f=0.0000	6.33	f=0.0000
Model 2	PBE	2.45	f=0.0005	3.31	f=0.0002	3.39	f=0.0006
	PBE0	3.92	f=0.0024	3.93	f=0.0014	3.96	f=0.0000
	HSE06	3.45	f=0.0004	3.89	f=0.0023	3.89	f=0.0000
	B3LYP	3.62	f=0.0006	3.83	f=0.0022	3.83	f=0.0000
	ωB97x-D	4.16	f=0.0094	4.28	f=0.0037	4.28	f=1.1449
Model 3	PBE	2.09	f=0.0001	2.09	f=0.0000	2.18	f=0.0003
	PBE0	2.73	f=0.0002	2.97	f=0.0002	3.68	f=0.0030
	HSE06	2.71	f=0.0002	2.95	f=0.0002	3.17	f=0.0002
	B3LYP	2.67	f=0.0001	2.92	f=0.0002	3.36	f=0.0005
	ωB97x-D	2.98	f=0.0002	3.17	f=0.0002	3.95	f=1.1949
Model 4	PBE	1.82	f=0.0000	2.06	f=0.0000	2.21	f=0.1274
	PBE0	2.90	f=0.2207	2.94	f=0.1239	3.12	f=0.0295
	HSE06	2.84	f=0.0002	2.84	f=0.2289	2.90	f=0.1499
	B3LYP	2.80	f=0.2315	2.87	f=0.1656	2.99	f=0.0036
	ωB97x-D	3.17	f=0.1405	3.17	f=0.0508	3.57	f=0.1089
Model 5	PBE	1.75	f=0.0001	1.89	f=0.0012	1.95	f=0.0000
	PBE0	2.74	f=0.0002	2.93	f=0.1465	3.14	f=0.0117
	HSE06	2.72	f=0.0001	2.74	f=0.0002	2.88	f=0.0007
	B3LYP	2.68	f=0.0002	2.86	f=0.1590	2.87	f=0.0211
	ωB97x-D	2.98	f=0.0002	3.17	f=0.0856	3.59	f=0.1083
Model 6	PBE	1.44	f=0.0000	1.62	f=0.0001	1.68	f=0.0000
	PBE0	2.74	f=0.0002	2.90	f=0.1208	2.91	f=0.0932
	HSE06	2.40	f=0.0000	2.59	f=0.0001	2.71	f=0.0001
	B3LYP	2.61	f=0.0001	2.68	f=0.0001	2.76	f=0.0017
	ωB97x-D	2.98	f=0.0002	3.17	f=0.1508	3.17	f=0.0407

S4 Frontier orbital visualisations

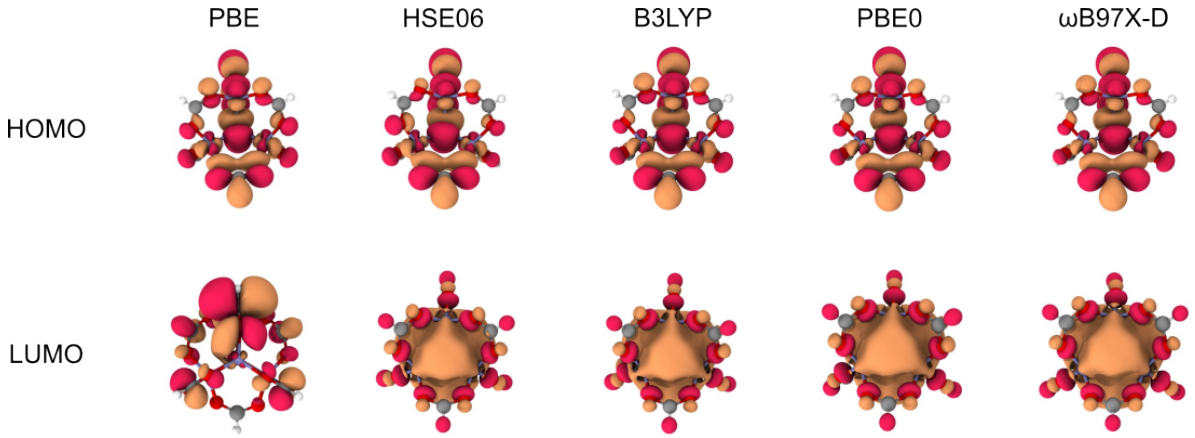

Figure S3: Model 1: Visualisation of the TDDFT/TZVP electron density (contour value of 0.02) of the HOMO and LUMO for each functional.

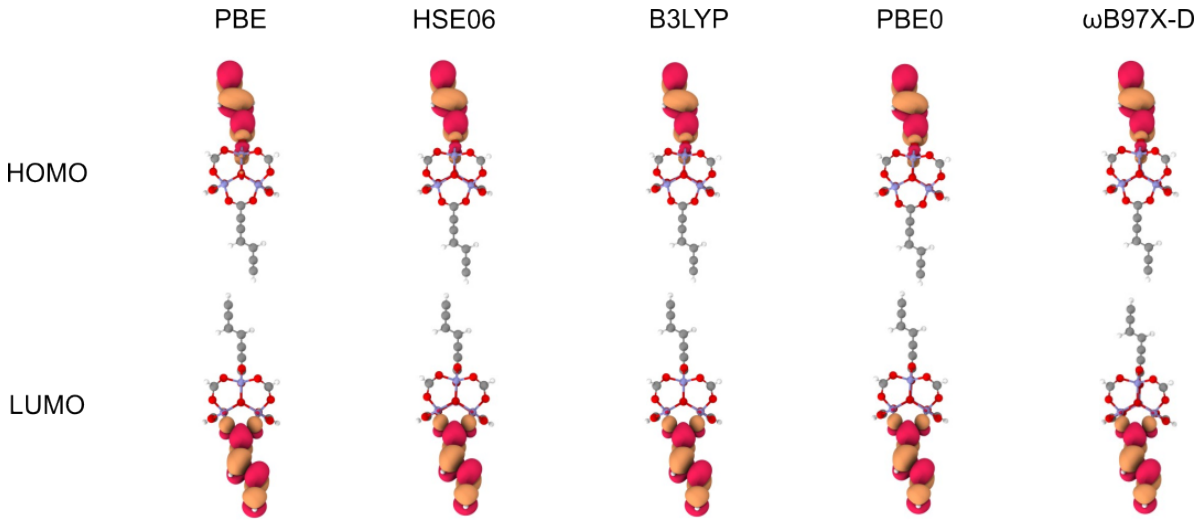

Figure S4: Model 2: Visualisation of the TDDFT/TZVP electron density (contour value of 0.02) of the HOMO and LUMO for each functional.

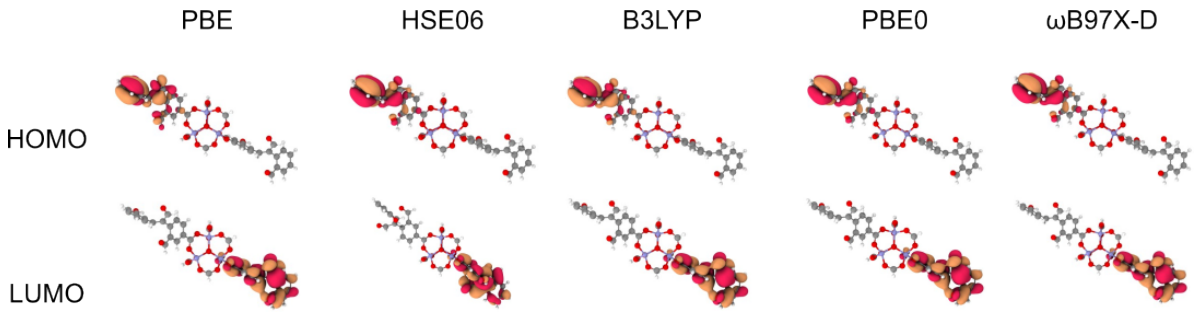

Figure S5: Model 3: Visualisation of the TDDFT/TZVP electron density (contour value of 0.02) of the HOMO and LUMO for each functional.

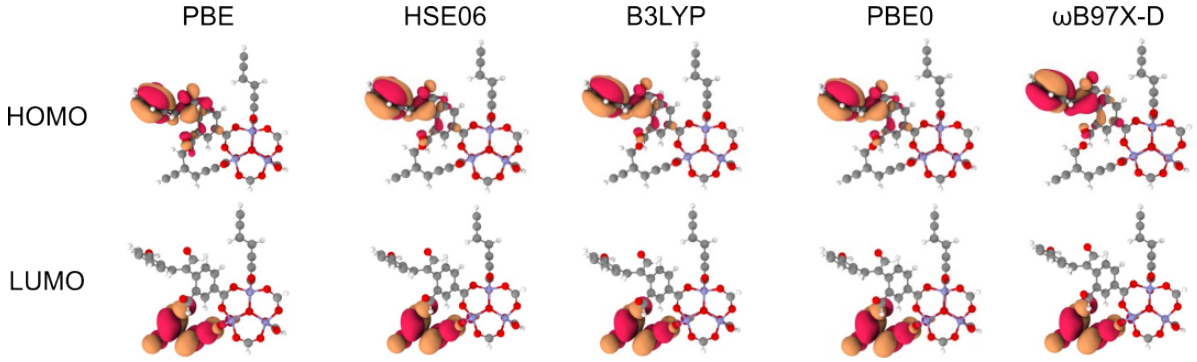

Figure S6: Model 4: Visualisation of the TDDFT/TZVP electron density (contour value of 0.02) of the HOMO and LUMO for each functional.

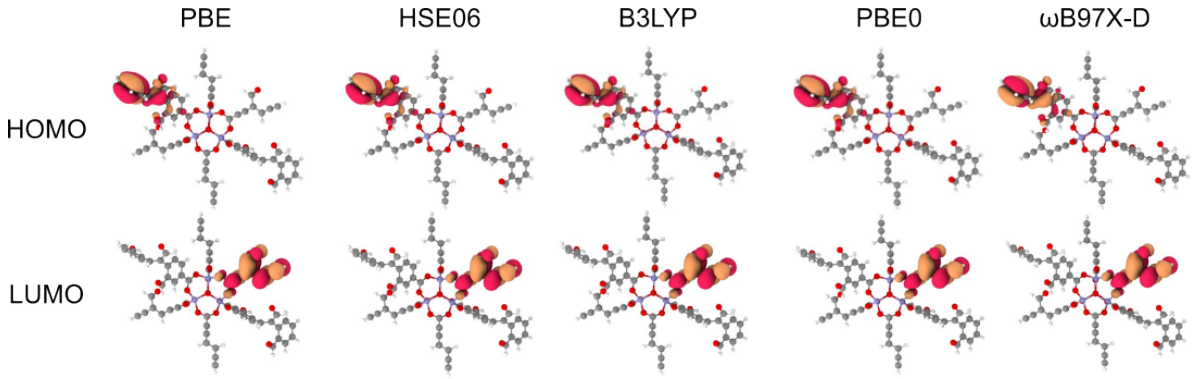

Figure S7: Model 5: Visualisation of the TDDFT/TZVP electron density (contour value of 0.02) of the HOMO and LUMO for each functional.

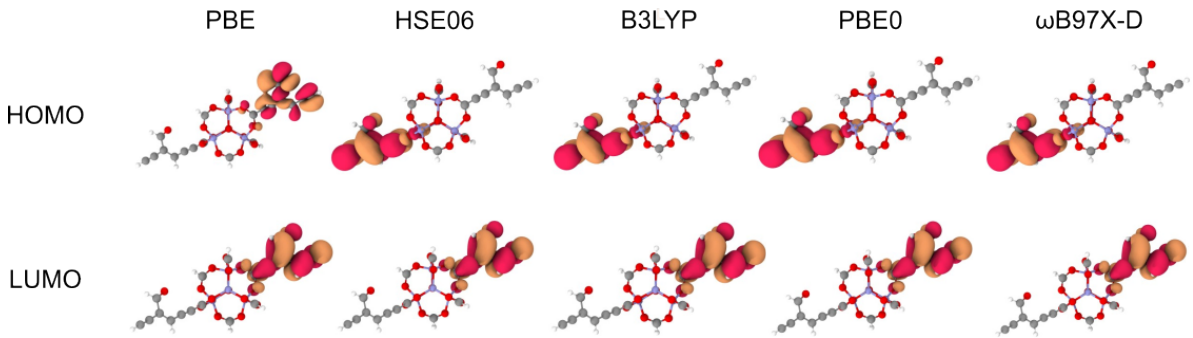

Figure S8: Model 6: Visualisation of the TDDFT/TZVP electron density (contour value of 0.02) of the HOMO and LUMO for each functional.

S5 Density differences

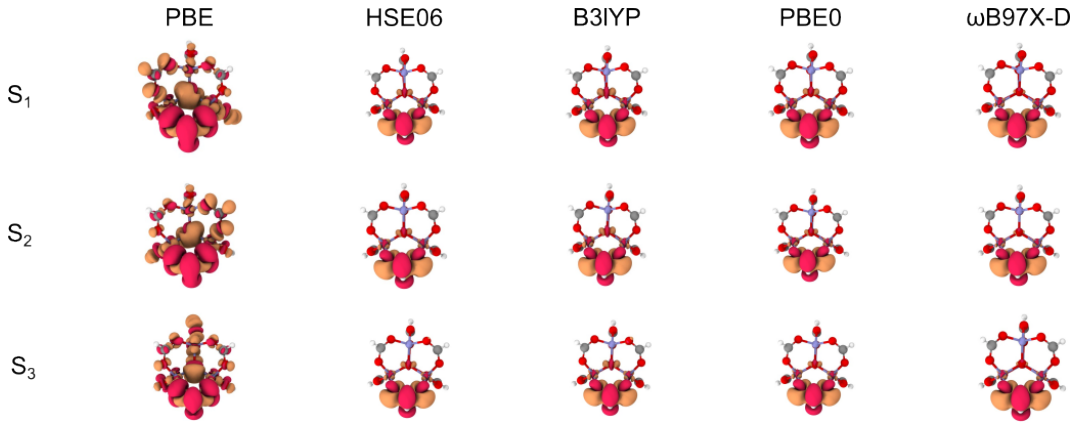

Figure S9: Model 1: Visualisation of the TDDFT/TZVP density difference (contour value of 0.0015) between the first (S_1), second (S_2), and third (S_3) excited states, and the ground (S_0) state for each functional.

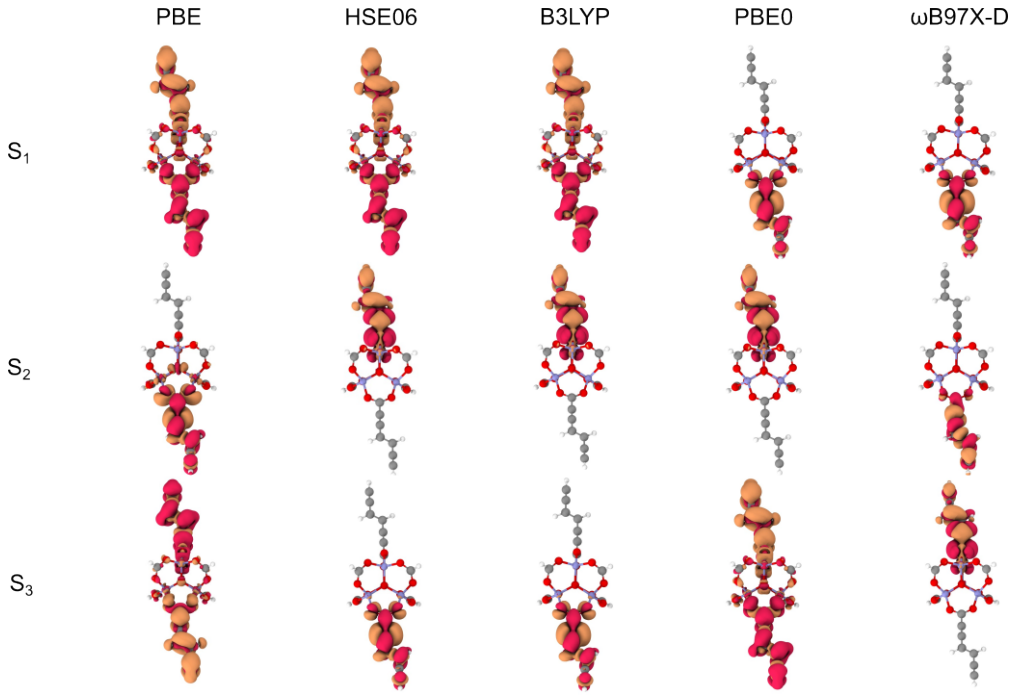

Figure S10: Model 2: Visualisation of the TDDFT/TZVP density difference (contour value of 0.0015) between the first (S_1), second (S_2), and third (S_3) excited states, and the ground (S_0) state for each functional.

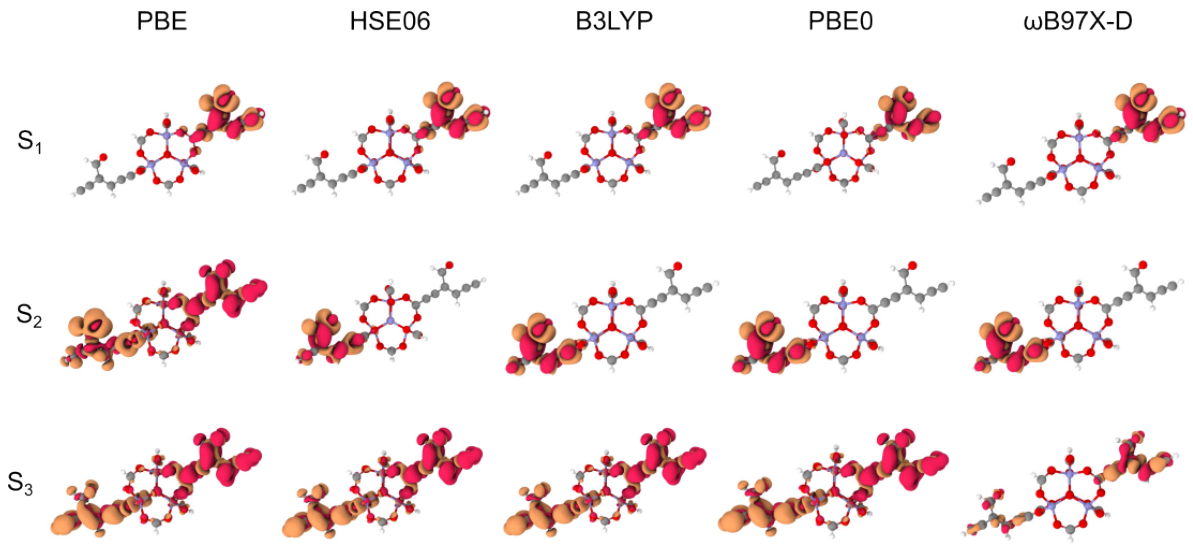

Figure S11: Model 3: Visualisation of the TDDFT/TZVP density difference (contour value of 0.0015) between the first (S_1), second (S_2), and third (S_3) excited states, and the ground (S_0) state for each functional.

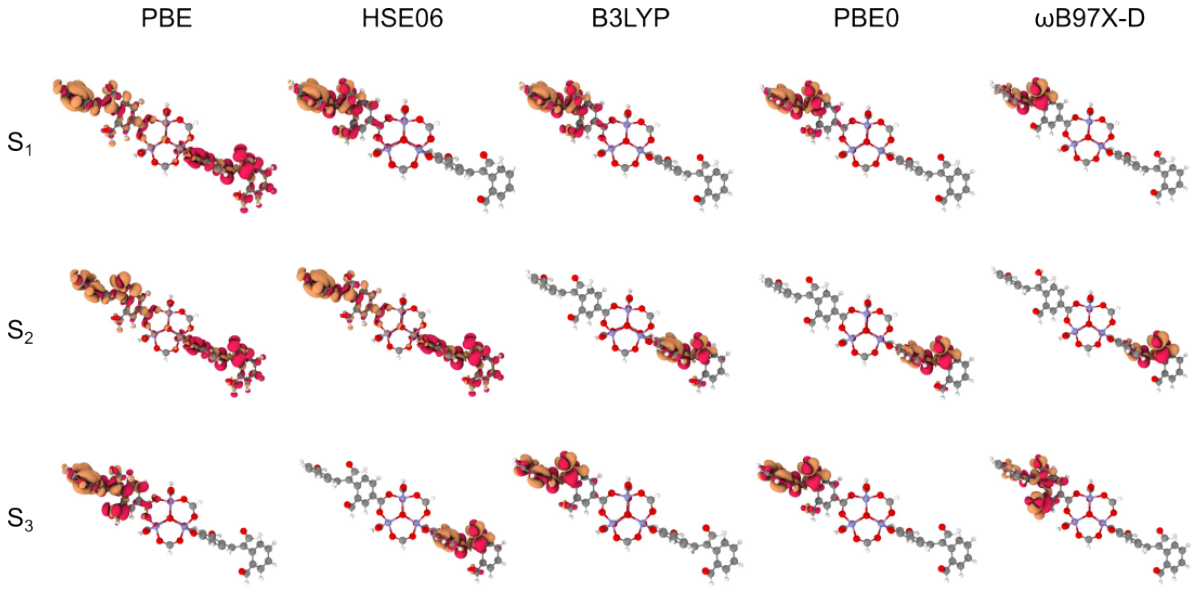

Figure S12: Model 4: Visualisation of the TDDFT/TZVP density difference (contour value of 0.0015) between the first (S_1), second (S_2), and third (S_3) excited states, and the ground (S_0) state for each functional.

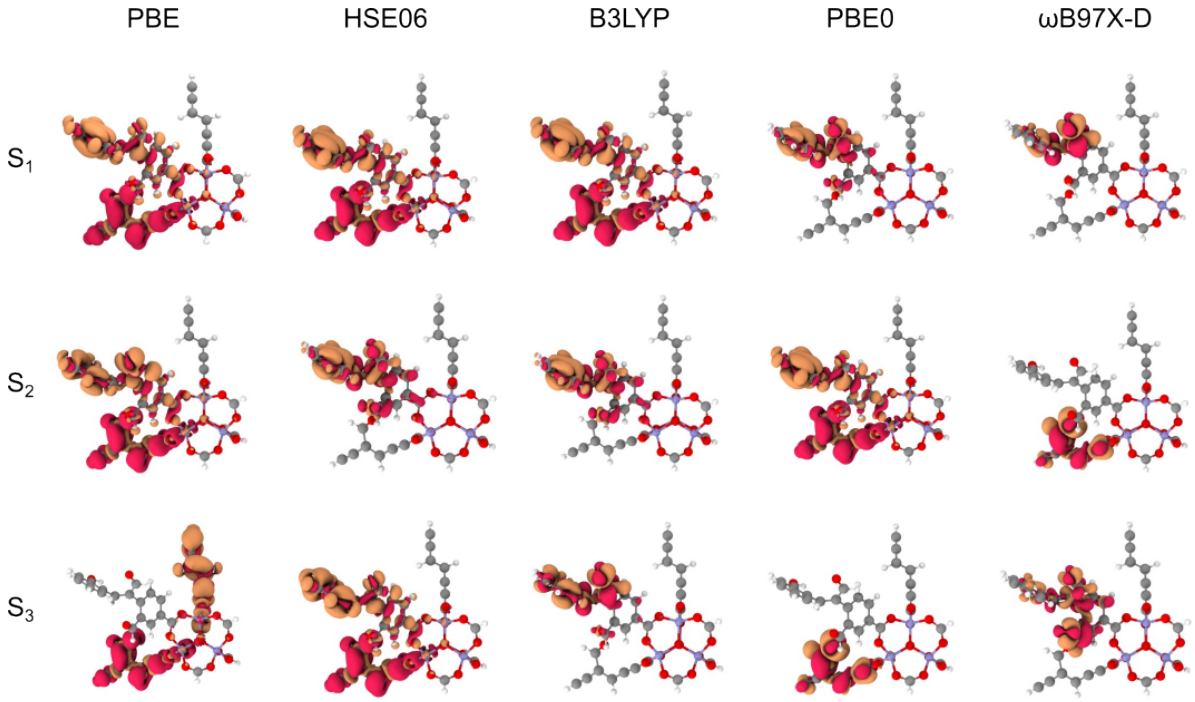

Figure S13: Model 5: Visualisation of the TDDFT/TZVP density difference (contour value of 0.0015) between the first (S_1), second (S_2), and third (S_3) excited states, and the ground (S_0) state for each functional.

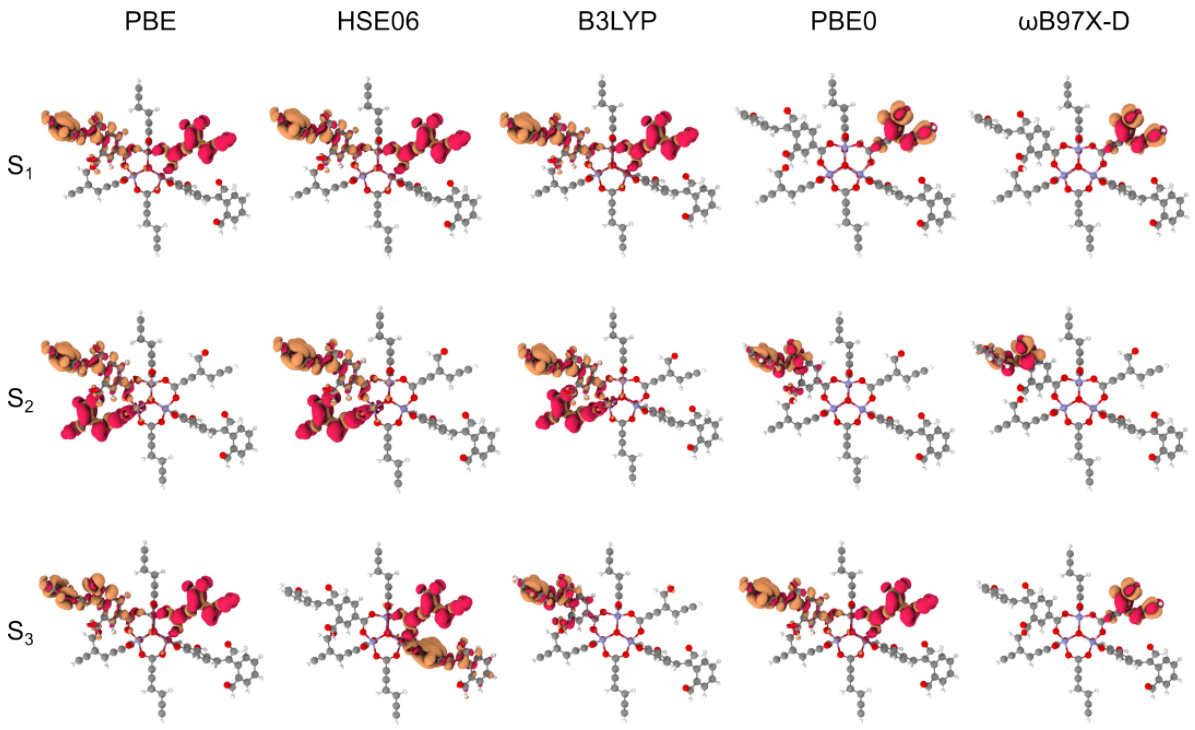

Figure S14: Model 6: Visualisation of the TDDFT/TZVP density difference (contour value of 0.0015) between the first (S_1), second (S_2), and third (S_3) excited states, and the ground (S_0) state for each functional.

References

[1] G. Kresse and J. Furthmüller, *Physical Review B*, 1996, **54**, 11169–11186.

[2] A. M. Ganose, A. J. Jackson and D. O. Scanlon, *Journal of Open Source Software*, 2018, **3**, 717.

[3] S. Dapprich, I. Komáromi, K. S. Byun, K. Morokuma and M. J. Frisch, *J. Mol. Structure: Theochem*, 1999, 1–21.

[4] C. F. Macrae, I. Sovago, S. J. Cottrell, P. T. A. Galek, P. McCabe, E. Pidcock, M. Platings, G. P. Shields, J. S. Stevens, M. Towler and P. A. Wood, *Journal of Applied Crystallography*, 2020, **53**, 226–235.

[5] M. J. Frisch, G. W. Trucks, H. B. Schlegel, G. E. Scuseria, M. A. Robb, J. R. Cheeseman, G. Scalmani, V. Barone, G. A. Petersson, H. Nakatsuji, X. Li, M. Caricato, A. V. Marenich, J. Bloino, B. G. Janesko, R. Gomperts, B. Mennucci, H. P. Hratchian, J. V. Ortiz, A. F. Izmaylov, J. L. Sonnenberg, D. Williams-Young, F. Ding, F. Lipparini, F. Egidi, J. Goings, B. Peng, A. Petrone, T. Henderson, D. Ranasinghe, V. G. Zakrzewski, J. Gao, N. Rega, G. Zheng, W. Liang, M. Hada, M. Ehara, K. Toyota, R. Fukuda, J. Hasegawa, M. Ishida, T. Nakajima, Y. Honda, O. Kitao, H. Nakai, T. Vreven, K. Throssell, J. A. Montgomery, Jr., J. E. Peralta, F. Ogliaro, M. J. Bearpark, J. J. Heyd, E. N. Brothers, K. N. Kudin, V. N. Staroverov, T. A. Keith, R. Kobayashi, J. Normand, K. Raghavachari, A. P. Rendell, J. C. Burant, S. S. Iyengar, J. Tomasi, M. Cossi, J. M. Millam, M. Klene, C. Adamo, R. Cammi, J. W. Ochterski, R. L. Martin, K. Morokuma, O. Farkas, J. B. Foresman and D. J. Fox, *Gaussian16, Revision A.03*, 2016.

[6] M. J. Frisch, G. W. Trucks, H. B. Schlegel, G. E. Scuseria, M. A. Robb, J. R. Cheeseman, G. Scalmani, V. Barone, G. A. Petersson, H. Nakatsuji, X. Li, M. Caricato, A. V. Marenich, J. Bloino, B. G. Janesko, R. Gomperts, B. Mennucci, H. P. Hratchian, J. V. Ortiz, A. F. Izmaylov, J. L. Sonnenberg, D. Williams-Young, F. Ding, F. Lipparini, F. Egidi, J. Goings, B. Peng, A. Petrone, T. Henderson, D. Ranasinghe, V. G. Zakrzewski, J. Gao, N. Rega, G. Zheng, W. Liang, M. Hada, M. Ehara, K. Toyota, R. Fukuda, J. Hasegawa, M. Ishida, T. Nakajima, Y. Honda, O. Kitao, H. Nakai, T. Vreven, K. Throssell, J. A. Montgomery, Jr., J. E. Peralta, F. Ogliaro, M. J. Bearpark, J. J. Heyd, E. N. Brothers, K. N. Kudin, V. N. Staroverov, T. A. Keith, R. Kobayashi, J. Normand, K. Raghavachari, A. P. Rendell, J. C. Burant, S. S. Iyengar, J. Tomasi, M. Cossi, J. M. Millam, M. Klene, C. Adamo, R. Cammi, J. W. Ochterski, R. L. Martin, K. Morokuma, O. Farkas, J. B. Foresman and D. J. Fox, *Gaussian09, Revision D.01*, 2016.

[7] S. G. Balasubramani, G. P. Chen, S. Coriani, M. Diedenhofen, M. S. Frank, Y. J. Franzke, F. Furche, R. Grotjahn, M. E. Harding, C. Hättig, A. Hellweg, B. Helmich-Paris, C. Holzer, U. Huniar, M. Kaupp, A. Marefat Khah, S. Karbalaei Khani, T. Müller, F. Mack, B. D. Nguyen, S. M. Parker, E. Perlt,

D. Rappoport, K. Reiter, S. Roy, M. Rückert, G. Schmitz, M. Sierka, E. Tapavicza, D. P. Tew, C. van Wüllen, V. K. Voora, F. Weigend, A. Wodyński and J. M. Yu, *The Journal of Chemical Physics*, 2020, **152**, 184107.

[8] W. Humphrey, A. Dalke and K. Schulten, *Journal of Molecular Graphics*, 1996, **14**, 33–38.